Desalination and Water Treatment
www.deswater.com

doi: 10.5004/dwt.2021.26758

215 (2021) 194–208
March

Enhancing adsorption of crystal violet dye through simple base modification of leaf adsorbent: isotherm, kinetics, and regeneration

Namal Priyantha[a], Amal Asheeba Romzi[b], Chin Mei Chan[b], Linda B. L. Lim[b,*]

[a]*Faculty of Science, Department of Chemistry, University of Peradeniya, Peradeniya, Sri Lanka, email: namal.priyantha@yahoo.com*
[b]*Chemical Sciences Programme, Faculty of Science, Universiti Brunei Darussalam, Jalan Tungku Link, Gadong BE 1410, Negara Brunei Darussalam, Tel. +673 8748010; emails: linda.lim@ubd.edu.bn (L.B.L. Lim), asheeba.romzi@gmail.com (A.A. Romzi), chinmei.chan@ubd.edu.bn (C.M. Chan)*

Received 2 June 2020; Accepted 1 November 2020

ABSTRACT

Dimorcarpus longan ssp. malesianus var. Malesianus (Mata Kuching) leaves (MKL) show a strong affinity toward crystal violet (CV), a commonly used industrial dye. Treatment of MKL with aqueous 1.0 M NaOH solution through stirring for 2.0 h, followed by washing and drying, enhances the adsorption of CV onto the modified adsorbent (NaOH-MKL), due to the conversion of acidic functional groups to the corresponding anionic forms leading to stronger Coulombic attractions. The performance of MKL and its modified NaOH-MKL toward CV dye adsorption indicates a strong attraction of both adsorbents. Strong adsorption of CV molecules to MKL and NaOH-MKL is evidenced by changes in the Fourier transform infrared spectroscopic peaks and scanning electron microscopic images upon interaction with the adsorbate. The Sips isotherm, among the five adsorption isotherm models used in this study, is suitable in explaining the interaction of both adsorbents with CV dye molecules. The maximum adsorption capacity (q_{max}) of NaOH-MKL adsorbent toward CV is 391.7 mg g^{-1} under optimum conditions according to the Sips adsorption isotherm, which is 88% enhancement over the unmodified MKL with q_{max} of 208.1 mg g^{-1}. Approach of CV dye molecules onto MKL/NaOH-MKL for adsorption is explained by the pseudo-second-order kinetics with an apparent rate constant of 6.108 g $mmol^{-1}$ min^{-1}, which is 72% increase over MKL. The superior nature of NaOH-MKL would make it an excellent sorbent for the removal of CV dye, which would thus have the potential for extrapolation toward real applications in the treatment of wastewater.

Keywords: Base modified leaf adsorbent; Adsorption isotherm; Crystal violet cationic dye; Kinetics; Regeneration

1. Introduction

Over the past couple of decades, adsorbents derived from agriculture [1,2], wood [3] and soil [4] materials, industrial wastes [5,6], food waste [7], and other natural substances [8,9] have been reported for the removal of toxic pollutants. Recent years have seen the emergence of cellulose derived adsorbents [10,11] as well as adsorbents that have been modified [12–14] or synthesized [15]. Further, sophisticated adsorbents, which required complicated methods of synthesis, do not necessary equate to high adsorption capacity toward pollutants. In many cases, reports have shown that natural adsorbents exhibit better adsorption capacity. For example, synthesized poly(acrylic acid)-halloysite nanoclay hydrogel, and *Ipomoea aquatica* (water spinach) roots, a natural adsorbent, exhibited adsorption capacity of 4.33 and 455.7 mg g^{-1}, respectively, toward Auramine O dye [16,17]. With the world's pollution problem

* Corresponding author.

intensifying at an alarming rate, the search for good, stable adsorbents that can remove pollutants effectively is at present still an on-going process.

Leaf-based adsorbents such as leaves of pomelo [18], tea [19], *C. camphora* [20], *Nepenthes rafflesiana* [21], *Artocarpus* spp. [22], and others [23] have attracted much attention as adsorbent materials due to several factors such as abundant availability, cheap, environmental friendly, and presence of various functional groups which could aid in the adsorption process [24]. Despite many reports on the potential utility of leaf-based adsorbents for the removal of toxic dyes, leaves of *Dimorcarpus longan* ssp. malesianus var. Malesianus, locally known as Mata Kuching leaves (MKL), have not been widely studied. To date, to the best of our knowledge, there has only been one report on the use of MKL as adsorbent for the removal of brilliant green dye [25].

The chosen adsorbate in this study is crystal violet (CV) dye, which is otherwise known as gentian violet or methyl violet 10B. Apart from being used as a synthetic dye in textile and food industries, CV can be applied to skin infection as an antiseptic, in biological staining, as antimycotic and antibacterial agent, etc. [26]. Despite its many uses, CV has its downside in that it is believed to be a clastogen, can cause headache and dizziness when ingested, and has shown to decrease white blood cell count [27]. Besides, experiments with mice indicated the dye to be carcinogenic [28].

This research is focussed on detailed investigation of the interaction of MKL with CV dye as well as chemical modification of MKL through the treatment of aqueous NaOH solution in order to determine if NaOH modified MKL (NaOH-MKL) could enhance its adsorption capacity toward CV. Studies of CV adsorption onto both MKL and NaOH-MKL were conducted using a wide range of experimental conditions such as effects of contact time, pH, and ionic strength. Adsorption equilibrium and kinetics aspects were undertaken on both MKL and NaOH-MKL and the experimental data were fitted with various models. Attempts on regeneration of these adsorbents were also investigated in order to provide insight into the reusability of these adsorbents.

2. Materials and methods

2.1. Chemicals and instrumentation

Crystal violet (CV) dye (formula: $C_{25}H_{30}N_3Cl$; molar mass: 407.98 g mol^{-1}) was purchased from Sigma-Aldrich (USA), and was used to prepare 1,000 mg L^{-1} stock solution. Adjustment of pH of solutions was done using 0.1 mol L^{-1} HCl and/or 0.1 mol L^{-1} NaOH. Sodium chloride (NaCl) and potassium nitrate (KNO_3) were used in the investigation of ionic strength and point of zero charge, respectively. All chemicals were used without further purification, and distilled water was used as the medium throughout the study.

Shimadzu UV-1601PC UV-visible spectrophotometer (Japan) was used for measuring the absorbance of CV dye solutions at the wavelength of 624 nm. Shimadzu IR Prestige-21 spectrophotometer (Japan) for Fourier transform infrared spectroscopy (FTIR) analysis was used for the identification of functional groups of MKL and NaOH-MKL through the KBr method. For the investigation of surface morphology of samples, scanning electron microscopy (SEM) JSM-7610F JEOL model (Japan) was used.

2.2. Sample preparation

D. longan ssp. malesianus var. Malesianus MKL, collected locally and shown as Fig. S1a, were first washed with distilled water to remove any surface dirt prior to drying to a constant mass in an oven at 60°C. The dried MKL (Fig. S1b) was then ground and blended into powder, followed by sieving using laboratory sieve apparatus. Particles of less than 355 μm were collected and kept in a sealed bag until ready to be used (Fig. S1c).

Chemical modification of MKL was affected by treatment of 20.0 g of MKL with 400 mL of 1.0 M of NaOH followed by stirring for 2.0 h. The mixture was filtered and the residue was then washed with distilled water to neutralize the pH of the modified MKL, and washing was continued until the pH became 7.0. Thereafter, NaOH-modified MKL was dried in oven at 60°C. The dried NaOH-MKL, shown as Fig. S1d, was kept in a sealed bag until ready to be used.

2.3. Optimization of parameters and batch adsorption experiments

Mass to volume ratio of the solid adsorbent and adsorbate solution was maintained at 1:500 throughout (i.e., 0.020 g of MKL or NaOH treated MKL with 10.0 mL of CV dye solution), unless otherwise stated. Suspensions were then shaken at ambient temperature at 250 rpm using the orbital shaker, except for thermodynamics studies which were carried out within the temperature range from 298 to 343 K. Investigation of the effects of contact time (30 min–4.0 h), pH (4–10), and ionic strength (0.1–1.0 M NaCl) on the extent of dye removal was carried out using 100 mg L^{-1} CV dye, following the methods of Zaidi et al. [22]. Adsorption kinetics studies were conducted using 100 mg L^{-1} CV solution. Batch adsorption isotherm experiments were performed with CV dye of concentration ranging from 0 to 1,000 mg L^{-1}.

After shaking each of the adsorbent-CV mixture for the required time, the solution was filtered and the absorbance of the dye filtrate was measured using UV-visible spectrophotometer. In addition, the absorbance of CV dye with concentrations ranging from 0 to 10 mg L^{-1} was also measured and a calibration curve was plotted in order to determine the dye filtrate concentration. The amount of dye adsorbed per unit mass of adsorbent (MKL or NaOH-MKL), q_e (mmol g^{-1}), was then calculated using Eq. (1) as shown below:

$$q_e = \frac{\left(C_i - C_e\right)V}{M_r m} \tag{1}$$

where C_i is the initial dye concentration (mg L^{-1}), C_e is the concentration of dye at equilibrium (mg L^{-1}), M_r is the molar mass of the CV dye (mol g^{-1}), V is the volume of dye solution (L), and m is the mass of adsorbent (g). The percentage removal of the dye was determined using:

$$\text{Percentage removal} = \frac{\left(C_i - C_e\right)}{C_i} \times 100 \tag{2}$$

2.4. Determination of point of zero charge

Determination of point of zero charge (pH_{pzc}) was done using 0.1 mol L^{-1} of KNO_3 solution following the method reported by Zehra et al. [29] within the range of pH from 2 to 10. The pH of the suspension of adsorbent was adjusted using 0.1 mol L^{-1} HCl and/or 0.1 mol L^{-1} NaOH. The pH-adjusted suspensions were then agitated for 24 h and the final pH was recorded.

2.5. Regeneration and reusability of adsorbents

All regeneration studies were conducted using 0.1 M NaOH, 0.1 M HCl, and distilled water, following the method as outlined by Zaidi et al. [22]. A control was also set up in which the spent adsorbent was reused without any prior treatment. The regeneration study was carried out for five consecutive cycles.

2.6. Error analysis

Suitability of isotherm and kinetics models for the adsorption system under investigation was investigated through the evaluation of error functions. The six error functions used in this study are the sum of absolute error (EABS), the average relative error (ARE), the Marquart's percentage standard deviation (MPSD), sum square error (SSE), hybrid fractional error function (HYBRID), and Chi-square test (χ^2), and they are represented in the Supplementary data by Eqs. (1)–(6), respectively. The smaller the error values, the better the fitted it is to the experiment data.

3. Results and discussion

3.1. Characterization of MKL and NaOH-MKL

3.1.1. Functional group characterization

Functional group characterization of MKL by FTIR spectroscopy indicates the presence of C–H (2,919 cm^{-1}), C=O (1,740 cm^{-1}), C=C of benzene (1,603 and 1,458 cm^{-1}), and C–H in-plane bending (1,034 cm^{-1}), as shown in Fig. 1 (top). Treatment of MKL with base shows prominent changes in the above peaks being shifted to 2,940; 1,734; 1,623; 1,465; and 1,031 cm^{-1}, respectively, suggesting that surface modification has taken place. Shifts in the peaks that appeared around 3,000 cm^{-1} can be attributed to changes in the chemical environment of –OH and groups, due to deprotonation of carboxylic acid groups during NaOH treatment of MKL. Base hydrolysis of ester groups would also occur during NaOH treatment leading to shift the stretching frequencies of –C=O groups. Lu et al. [30] also reported shifts to these functional groups in their studies when they chemically modified pomelo leaves with NaOH. It has also been reported that alkali treatment disrupts the structure of lignin allowing the structural linkages between lignin and carbohydrates to be separated [31]. This separation of linkage, which would be expected in NaOH-MKL, would favor interaction between the adsorbent and CV molecules.

In order to evaluate the functional groups that may be involved in the removal of CV, shifts of peaks in these functional groups provide a good indication. It is apparent in Fig. 1 (top) that peaks at 2,919; 1,740; 1,603; 1,517 cm^{-1} are shifted to 2,943; 1,735; 1,624; 1,508 cm^{-1}, respectively. Further, the peak intensities in the regions between 1,034–1,370 cm^{-1} and 512–894 cm^{-1} appeared different upon CV adsorption. Similar peak shifts are also observed in NaOH-MKL after CV dye adsorption.

3.1.2. Surface morphology of MKL and NaOH-MKL

Chemical treatment of MKL using 1.0 M NaOH shows that the adsorbent's surface morphology undergoes a drastic change, as shown by Figs. 2a and b, respectively. Prior to surface modification, MKL appears more compact and irregular. Base modification results in its surface becoming less dense, and even though the surface still remains highly irregular, more cavities and holes can be seen. Similar observations have been reported for other adsorbents such as rock melon skin whereupon the surface became more porous when the adsorbent was treated with NaOH [12]. Adsorption of CV onto the surface of both adsorbents results in the surface becoming less irregular and more flat, especially for MKL as shown in Fig. 2c. As for NaOH-MKL, large cavities are no longer obvious confirming coverage by dye molecules, as depicted in Fig. 2d.

3.1.3. Point of zero charge of MKL and NaOH-MKL

The pH_{PZC} is the pH at which there is net zero charge on the surface of an adsorbent, and it is an important aspect in surface science. This information is valuable in terms

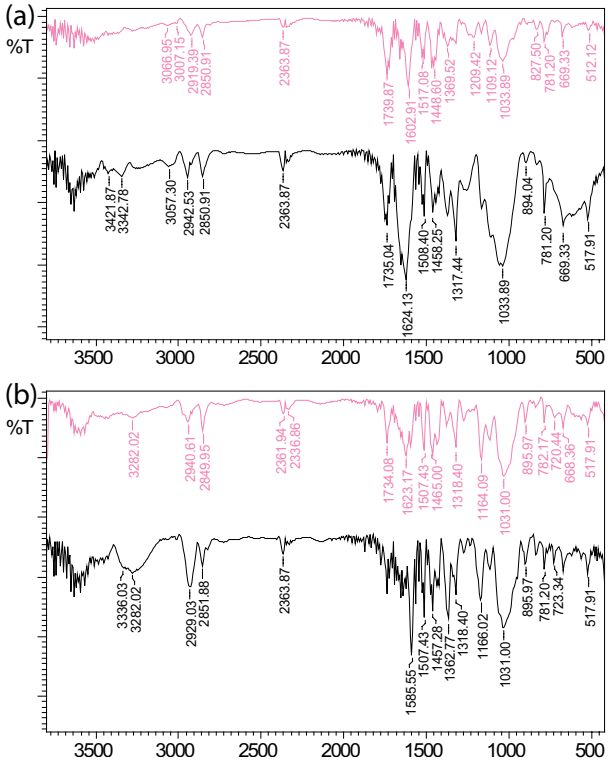

Fig. 1. FTIR spectra of MKL (a) and NaOH-MKL (b), before (pink) and after (black) adsorption of CV.

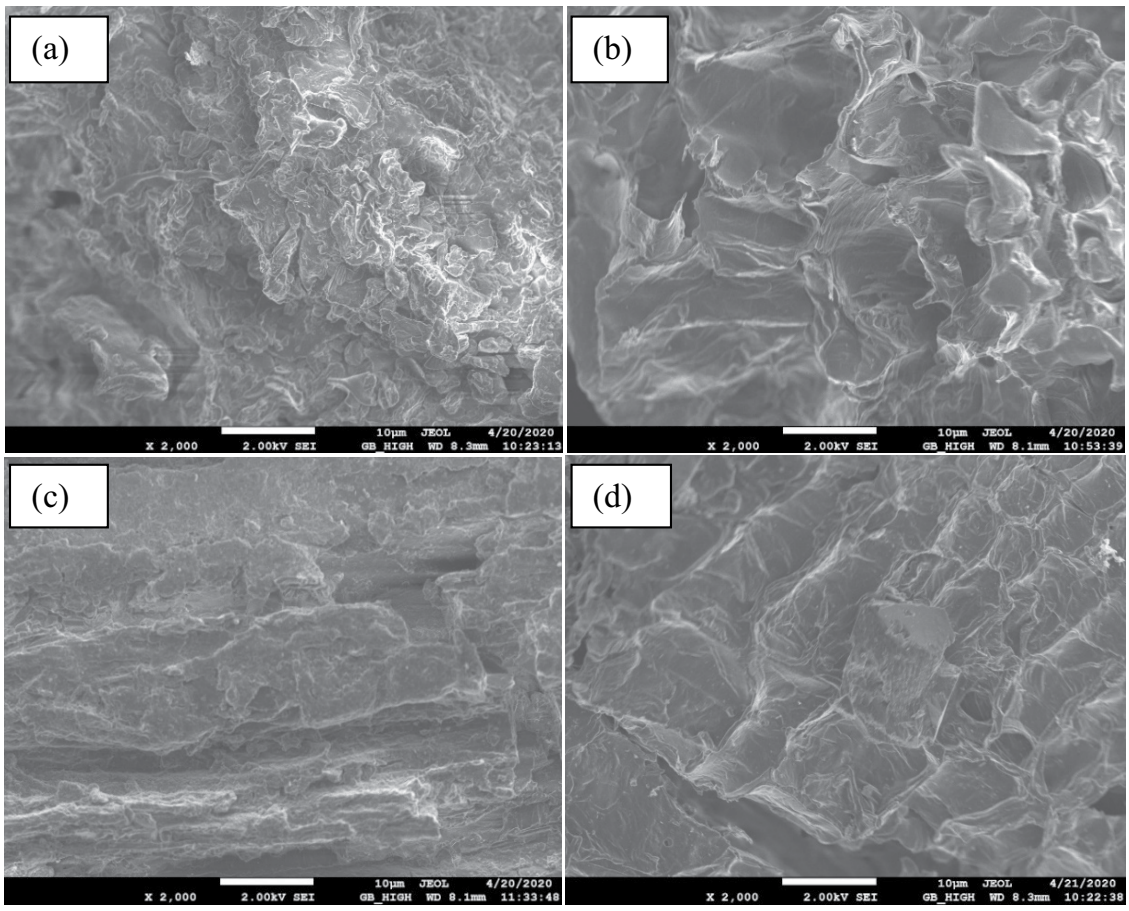

Fig. 2. SEM images of (a) MKL, (b) NaOH-MKL, (c) MKL-CV, and (d) NaOH-MKL-CV at ×2,000 magnification with the white scale bar representing 10 μm.

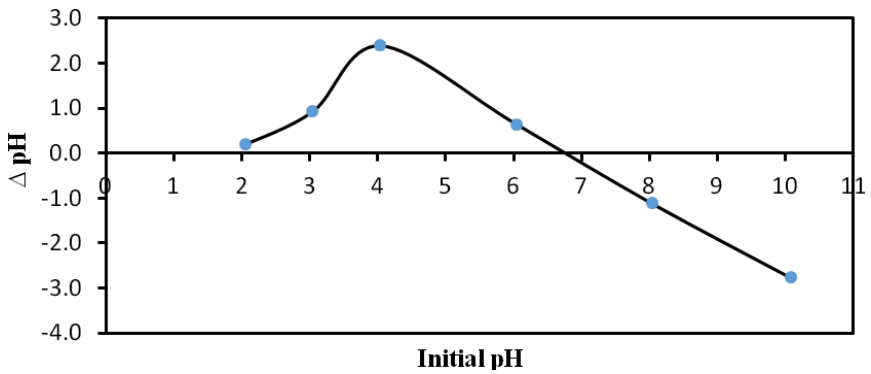

Fig. 3. Change in pH of NaOH-MKL suspension with initial for the determination of pH_{PZC}.

of forecasting how an adsorbent in various medium pH is likely to behave and adsorb toward a particular adsorbate. The pH_{PZC} of MKL was previously reported at pH 4.69 [23]. When subjected to base treatment, the pH_{PZC} of NaOH-MKL is found to be shifted to higher pH at 6.78 (Fig. 3). This observation could be attributed to deprotonation of the surface functional groups as a result of base treatment, thereby causing the surface of the adsorbent to become more basic [30]. Similar shifts of pH_{PZC} to higher pH were also reported for NaOH modified adsorbents such as cassava peel [32] and *Azolla pinnata* [33].

3.1.4. Thermogravimetric analyses of MKL and NaOH-MKL

Increase in the porous nature of MKL when treated with NaOH solution is further supported by variation of the mass percentage with firing temperature in thermogravimetric analyses (TGA) experiments. Water molecules

trapped within the matrix of the adsorbent can easily be vaporized when pores are exposed as a result of NaOH treatment, which is represented by the first mass reduction step in the TGA curve, shown in Fig. 4, and the evaporation of moisture is observed to be completed when the furnace temperature reaches little over 100°C as clearly evident in the TGA curve. As pores are not much exposed in untreated MKL, loss of moisture takes place gradually up to higher temperatures. The second sharp drop of mass reduction in the TGA curve of NaOH-MKL is due to loss of organic matter, and this process continues up to about 600°C. Although a similar mass reduction is observed in the TGA curve of untreated MKL, this step is also not as sharp as that of NaOH-MKL due to the same reason explained above, that is, lack of exposed pores. Nevertheless, the total mass reduction at the firing temperature of 700°C as compared to that at the initial temperature is the same for both MKL and NaOH-MKL, indicating the complete loss of moisture and organic matters from both types of adsorbents at the end of the thermogravimetric experiment.

3.2. Optimization of adsorption parameters

3.2.1. Effect of contact time

A crucial parameter in adsorption study is the period of time required for an adsorbent–adsorbate system to reach equilibrium. This allows the proper planning and cost evaluation of operating conditions. Some adsorbents, owing to their nature, require longer time to reach equilibrium than others. Fig. 5 shows that both MKL and NaOH-MKL are able to remove 64% and 92% CV dye, respectively, under ambient conditions within the first 30 min. The initial availability of vacant active sites allows the CV dye molecules to be more efficiently interacted and deposited onto the adsorbent's surface. Thereafter, the uptake of CV does not seem to be much changed, reaching a plateau at 2.0 and 3.0 h for MKL and NaOH-MKL, respectively, indicating the establishment of the state of equilibrium. Therefore, a period of 2.0 and 3.0 h was selected as the optimum contact time for MKL and NaOH-MKL, respectively. About 50% more removal of CV by NaOH-MKL compared to untreated MKL is indicative of improved adsorption efficiency upon NaOH modification. This is probably due to stronger Coulombic attraction between positively charged CV molecules and negatively charged functionalities of the adsorbent which would have been formed during NaOH treatment as indicated through FTIR spectroscopic observations.

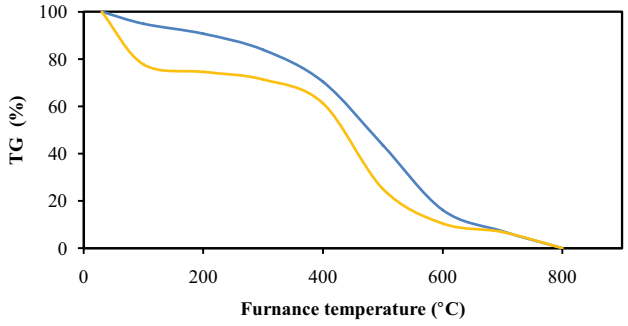

Fig. 4. TGA of MKL (—) and NaOH-MKL (—).

3.2.2. Effect of pH on adsorption of CV on MKL and NaOH-MKL

As wastewater contains many different types of pollutants, its pH is usually not at the neutral value. The pH of medium is an important parameter because it affects the charge on an adsorbent's surface, which in turn would alter its adsorption characteristics toward an adsorbate. It has been reported that many adsorbents change their adsorption efficiencies when medium pH is altered [34–36]. Investigation into the effect of medium pH on the adsorption of CV on both MKL and NaOH-MKL showed that prior to any pH adjustments, the extent of removal are 67% and 96%, respectively, at the optimum contact time (Fig. 6). MKL exhibited stability and maintained similar adsorption of 100 mg L^{-1} dye over the range of pH studied. NaOH-MKL, on the other hand, generally demonstrated higher adsorption capacity (>90% removal of CV) compared to the untreated adsorbent, except at strongly acidic medium of pH = 2. High concentration of H_3O^+ at pH 2 would lead to electrostatic attraction toward the negatively charged surface of NaOH-MKL, blocking CV dye molecules approaching the adsorbent's surface. Although it was expected that CV dye molecules being positively charged would show stronger attraction at pH > pH_{PZC} = 6.78, both MKL and NaOH-MKL demonstrated stability in varying medium pH, showing almost constant extent of removal except for pH 2. The highest removal of CV dye by MKL and NaOH-MKL was observed at pH 4 and 8, respectively. However, when compared to unadjusted pH, the difference in CV removal at optimum pH was only higher by <3% for both adsorbents. Therefore, no pH adjutment is necessary for efficient removal of CV by both adsobents, MKL and NaOH-MKL. This is an attractive feature since potential adsorbents in wastewater treatment application favors ability to remain stable in varying environmental conditions. Such adsorbents would effectively be used under different pH conditions of industrial effluents, and yet at the same time retain adsorption capacity and reduce operational cost.

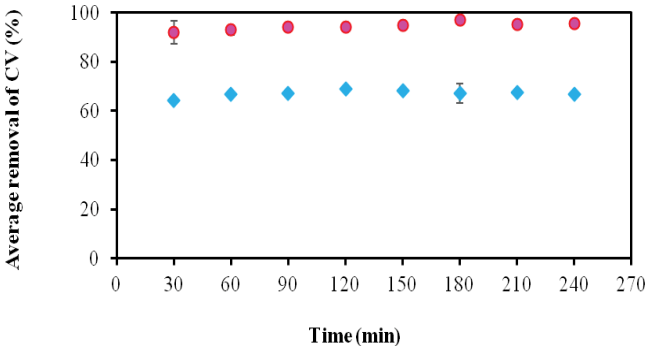

Fig. 5. Extent of removal of CV with contact time of MKL (◆) and NaOH-MKL (●) at ambient temperature and pH (0.020 g of MKL/NaOH-MKL with 10.0 mL of 100 mg L^{-1} CV dye).

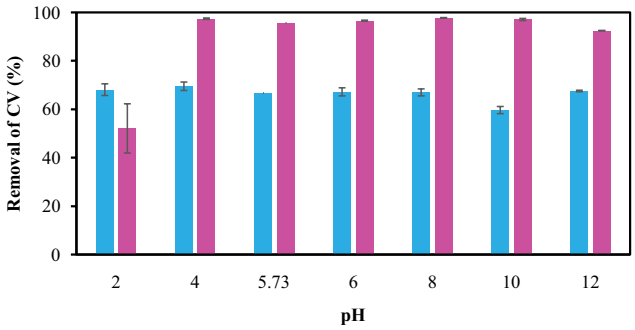

Fig. 6. Effect of pH on MKL (■) and NaOH-MKL (■) under ambient temperature condition (0.020 g of MKL/NaOH-MKL with 10.0 mL of 100 mg L^{-1} CV dye).

3.2.3. Effect of ionic strength on adsorption of CV on MKL and NaOH-MKL

It is imperative to perform effects of ionic strength in adsorption studies since wastewater discharged from industrial effluents contain various salts. The presence of different electrolytes can affect the ability of an adsorbent to adsorb adsorbates either by impeding its removal at higher ionic strength or causing it to maintain or even enhance its removal [37]. Some adsorbents have been known to result in aggregation when the ionic strength is increased. A common salt, NaCl, being often in use in textile industry to help enhance affinity of dyestuff toward fiber and to speed up the fixation of dye onto the material, was chosen as the model salt to be investigated in this study. It is also the main salt used in home water softeners. Of the two adsorbents, MKL shows its ability to maintain adsorption toward CV dye in the presence of different salt concentrations, with an approximately 16% increase in 1.0 M NaCl solution as shown in Fig. 7. The ionic environment containing Cl^- ions would probably promote the affinity of the adsorbent toward positively charged CV dye molecules.

NaOH-MKL, on the other hand, shows a reduction of approximately 26% when the salt concentration was increased to 1.0 M. As NaOH-MKL consists of Na^+ as the counter ion, introduction of NaCl would not interact with the adsorbent, and it would create an ionic environment surrounding adsorbent particles, thereby blocking adsorbate species to come in contact. This masking effect would become more significant as the concentration of NaCl increases as observed. Decrease in the extent of CV dye removal with increase in NaCl concentration is thus explained. However, detailed investigation of the variation of the strength of interaction of CV dye with MKL modified with different chemical agents in different types of ionic environments would be needed to arrive at a sound conclusion.

The stability demonstrated by MKL in varying ionic strengths, whilst maintaining great efficiency in CV removal (>90%) at 1.0 M NaCl, is an attractive feature in wastewater treatment application. This clearly indicates that MKL could be a potential low-cost adsorbent to be utilized. Even though NaOH-MKL shows decreased removal of CV at 1.0 M NaCl, its adsorption toward CV was still significant showing a value of 70%.

3.3. Adsorption kinetics of CV on MKL and NaOH-MKL

An important aspect in designing wastewater treatment plant is knowledge of adsorption kinetics. The rate of adsorption would help in the decision of whether the adsorbent is economically viable. In this study, two kinetics models, namely, the Lagergren pseudo-first-order model [38] and the pseudo-second-order model [39], were employed to provide insight into the adsorption kinetics of MKL and NaOH-MKL toward CV. The linearized equations of the two models are shown below:

Lagergren pseudo-first-order model:

$$\log\left(q_e - q_t\right) = \log q_e - \frac{t}{2.303}k_1 \tag{3}$$

Pseudo-second-order model:

$$\frac{t}{q_t} = \frac{1}{q_e^2 k_2} + \frac{t}{q_e} \tag{4}$$

where q_t is the amount of adsorbate adsorbed per gram of adsorbent (mmol g^{-1}) at time t (min), k_1 and k_2 are the pseudo-first-order rate constant (min^{-1}) and pseudo-second-order rate constant (g $mmol^{-1}$ min^{-1}), respectively.

Linear plots of data using these two models showed that higher R^2 (close to unity) and lower error values were derived from the pseudo-second-order model for both the

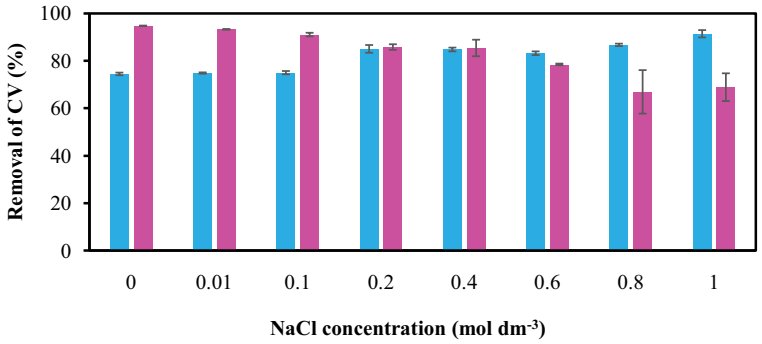

Fig. 7. Effect of ionic strength using NaCl on the adsorption of CV onto MKL (■) and NaOH-MKL (■) (ambient pH, 0.020 g of MKL/NaOH-MKL with 10.0 mL of 100 mg L^{-1} CV dye).

adsorbents, as shown in Fig. 8 and Table 1. Comparison of the experimental kinetics data with the simulated plots of both models in Fig. 9 further confirms the pseudo-second-order fitted closer, while large deviation was observed for the Lagergren pseudo-first-order kinetics. Another indication of the fitting of the pseudo-second-order kinetics stems from the close proximity between the adsorption capacity of the calculated (q_{calc}) vs. experimental (q_{exp}), whose values are shown in Table 1.

Based on pseudo-second-order kinetics, the adsorption rate for MKL and NaOH-MKL was 3.55 and 6.11 g mmol^{-1} min^{-1}, respectively. This shows that chemical modification of MKL has increased the rate of adsorption toward CV by almost 72%. Fast adsorption rate is one of the key factors when considering an adsorbent's application in wastewater treatment, as this will help reduce operation cost.

The validity of the Weber–Morris intraparticle diffusion model having three linear segments of the plots of q_t vs. $t^{1/2}$ with different slopes for both MKL and NaOH-MKL is indicative of three steps for adsorption: (1) rapid diffusion of CV molecules onto the surface of adsorbents; (2) intraparticle diffusion which could be the rate-limiting step; and (3) establishment of equilibrium (Fig. 10). The intercept

Table 1
Information of the Lagergren pseudo-first-order and pseudo-second-order kinetics models and their error values

Kinetics parameters	MKL	NaOH-MKL
Pseudo-first-order		
k_1 (min^{-1})	0.041	0.021
q_{calc} (mmol g^{-1})	0.0329	0.0202
R^2	0.8960	0.6697
ARE	91.076	109.167
SSE	0.050	0.176
HYBRID	4.107	9.354
EABS	1.011	1.905
MPSD	90.308	107.354
χ^2	0.780	1.777
Pseudo-second-order		
k_2 (g mmol^{-1} min^{-1})	3.554	6.108
q_{calc} (mmol g^{-1})	0.0849	0.1138
R^2	0.9994	0.9998
ARE	8.436	2.360
SSE	0.001	0.000
HYBRID	0.073	0.010
EABS	0.075	0.039
MPSD	14.498	3.676
χ^2	0.014	0.002
q_{calc} (mmol g^{-1})	0.0737	0.1032

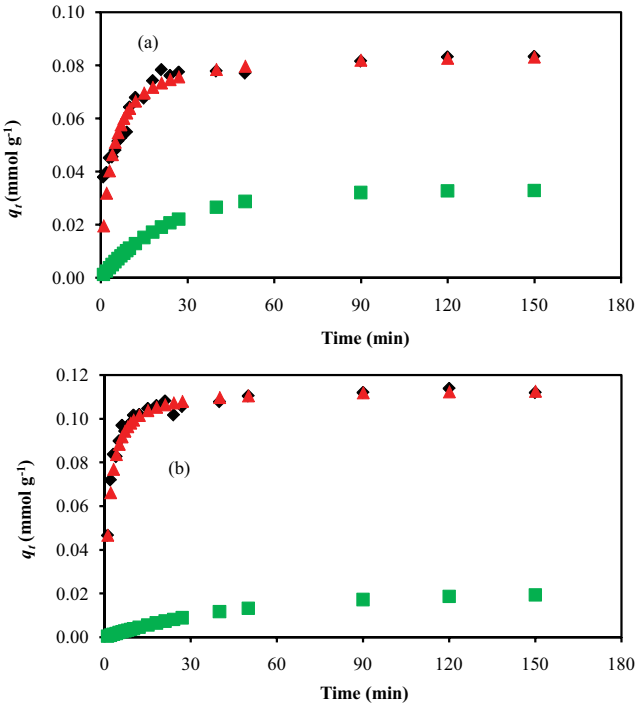

Fig. 9. Comparison of experimental data (◆) with simulated plots of the Lagergren pseudo-first-order (■) and pseudo-second-order (▲) of (a) MKL and (b) NaOH-MKL.

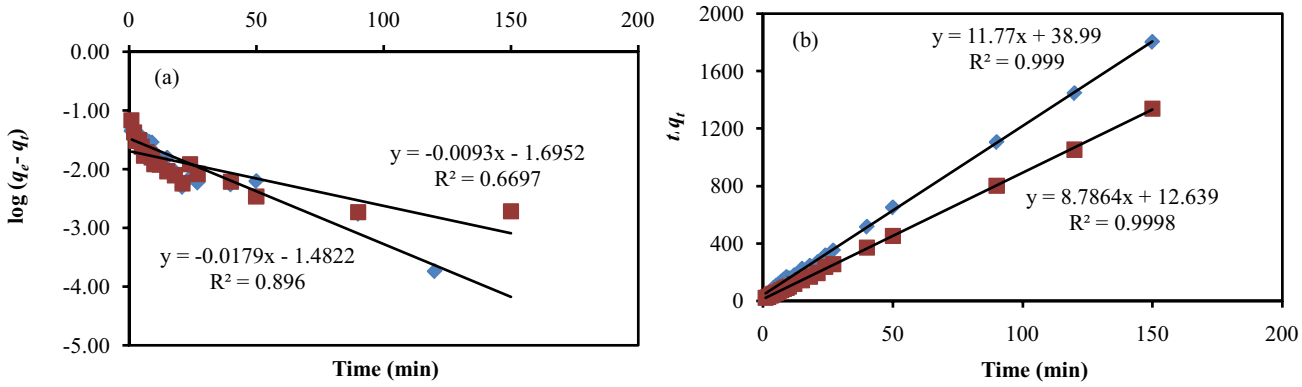

Fig. 8. Linear plots of (a) Lagergren pseudo-first-order and (b) pseudo-second-order kinetics models for the adsorption of CV onto MKL (◆) and NaOH MKL (■).

of q_t vs. $t^{1/2}$ plots is a measure of the boundary layer thickness. According to Fig. 10, the positive value of the intercept for both adsorbents is evident of having favorable conditions for biosorption, as observed throughout this research [40].

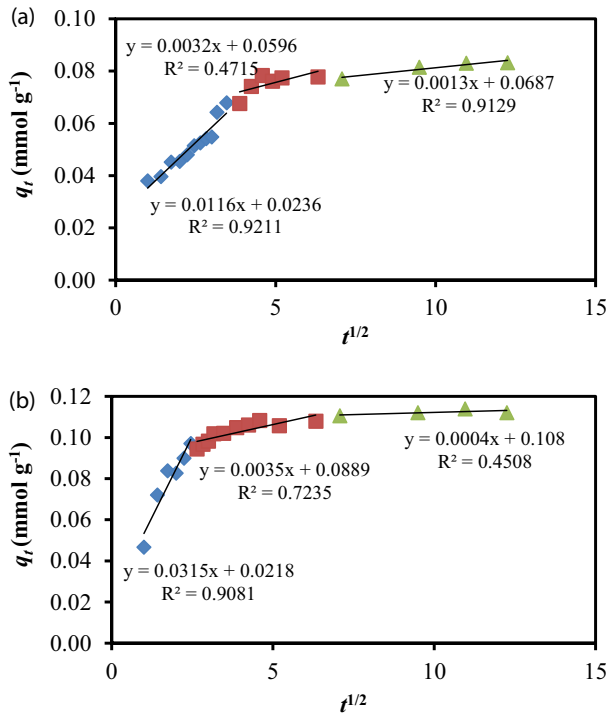

Fig. 10. Weber–Morris intraparticle diffusion plots for adsorption of CV onto (a) MKL and (b) NaOH-MKL.

3.4. Investigation of adsorption isotherms

Various isotherm models have been established over the years to help shed light onto equilibrium adsorption of a given adsorbent–adsorbate system [41,42]. Information derived from adsorption isotherm is of utmost importance toward the successful designing of wastewater treatment plant. Herein, five adsorption isotherm models, namely, Langmuir [43], Freundlich [44], Temkin [45], Redlich–Peterson (R–P) [46], and Sips [47], were deployed to test the experimental isotherm data of the adsorption system under investigation (Table 2).

Comparison of non-linear curve fitting of experimental isotherm data on adsorption of CV dye on MKL and NaOH-MKL with simulated curves of the above five isotherms is shown in Fig. 11, while isotherm constants together with error function values are shown in Tables 3 and 4, respectively. According to regression coefficient values, adsorption of CV on MKL could be explained by the Langmuir, Freundlich, and the Sips isotherms, while that on NaOH-MKL can be explained by the Langmuir and Sip isotherms. Further, magnitudes of error functions of MKL for both the Langmuir and Sip isotherms are about the same, while those of NaOH-MKL for the Langmuir isotherm are larger. Therefore, by considering both regression analysis and error function determinations, the Sips adsorption isotherm can be regarded to be the most suitable. The Sips isotherm, a combined form of the Langmuir and Freundlich models, is suitable for describing heterogeneous adsorption systems within a wide range of activities [48]. Further, the q_{max} values of 208.1 and 391.7 mg g^{-1} for MKL and NaOH-MKL, respectively, determined from the Sips isotherm can be considered to be representative values.

Table 2
Isotherm models used in this study

Isotherm models	Symbols
Langmuir: $\frac{C_e}{q_e}=\frac{1}{K_L q_{max}}+\frac{C_e}{q_{max}}$	K_L is the Langmuir constant (L $mmol^{-1}$); q_{max} and q_e are maximum adsorption capacity and adsorption capacity at equilibrium, respectively, both in mmol g^{-1}; C_e (mg L^{-1}) is the adsorbate concentration at equilibrium.
Freundlich: $\log q_e=\frac{1}{n}\log C_e+\log K_F$	K_F is the Freundlich constant [mmol g^{-1} (L $mmol^{-1})^{1/n}$]; n depicts the favourability of adsorption.
Temkin: $q_e=\left(\frac{RT}{b_T}\right)\ln K_T+\left(\frac{RT}{b_T}\right)\ln C_e$	K_T is the equilibrium binding constant (L $mmol^{-1}$); b_T is the Temkin constant; R is the gas constant (J K^{-1} mol^{-1}); T is the temperature (K).
Redlich–Peterson: $\ln\left(\frac{K_R C_e}{q_e}-1\right)=n\ln C_e+\ln a_R$	K_R (L g^{-1}) and a_R (L $mmol^{-1}$) are the R–P constants.
Sips: $\ln\left(\frac{q_e}{q_{max}-q_e}\right)=\frac{1}{n}\ln C_e+\ln K_s$	K_s is the Sips constant (L $mmol^{-1}$).

One of the important criteria in determining whether an adsorbent is suitable to be applied in wastewater treatment is its ability to effectively remove adsorbate. The higher the adsorption capacity of a given adsorbent, the more favorable it will be since this equates as being efficacious and lower cost. For this reason, it is imperative to compare the maximum adsorption capacity (q_{max}) of an adsorbent with other reported adsorbents prior to deciding its suitability in wastewater treatment applications. Herein, being a leaf-based adsorbent, the q_{max} of MKL was therefore initially compared with other leaf adsorbents for the removal of CV dye. Its superiority toward CV, compared to most leaf adsorbents, is clearly displayed in Table 5. Modification of MKL enhanced its q_{max} by 88% to 391.7 mg g^{-1}, a value higher than many adsorbents including those modified or synthesized, as shown in Table 5.

3.5. Thermodynamics studies

Variation of the amount of CV adsorbed with the initial concentration of CV at different temperatures is shown in Fig. 12 for both MKL and NaOH-MKL. Such

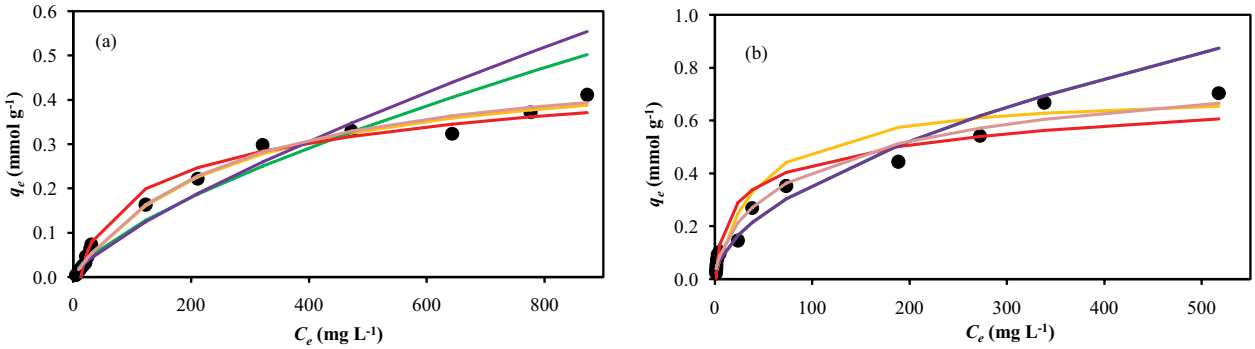

Fig. 11. Experiment isotherm data (●) with simulated plots of Langmuir (—), Freundlich (—), Temkin (—), R–P (—), and Sips (—) models for (a) MKL and (b) NaOH-MKL [Freundlich and R–P overlap in (b)].

Table 3
Isotherm results and error values based on different isotherm models for adsoption of CV dye on MKL

Model	Values	ARE	SSE	HYBRID	EABS	MPSD	χ^2
Langmuir		11.10	0.00	0.13	0.16	15.46	0.14
q_{max} (mmol g^{-1})	0.503						
q_{max} (mg g^{-1})	205.2						
K_L (L $mmol^{-1}$)	0.004						
R^2	0.9685						
Freundlich		20.82	0.03	0.69	0.48	26.48	0.21
K_F (mmol g^{-1} (L $mmol^{-1})^{1/n}$)	0.005						
n	1.438						
R^2	0.9500						
Temkin		35.09	0.01	1.19	0.29	84.63	0.94
K_T (L $mmol^{-1}$)	0.080						
b_T (kJ/mol)	28.306						
R^2	0.9761						
Redlich–Peterson		20.80	0.06	1.28	0.62	27.02	0.26
K_R (L g^{-1})	0.600						
β	0.242						
a_R (L $mmol^{-1}$)	184.14						
R^2	0.5677						
Sips		11.03	0.00	0.14	0.16	15.95	0.13
q_{max} (mmol g^{-1})	0.510						
q_{max} (mg g^{-1})	208.1						
K_s (L $mmol^{-1}$)	0.004						
$1/n$	1.004						
n	0.996						
R^2	0.9843						

Table 4
Isotherm results and error values based on different isotherm models for adsoption of CV dye on NaOH-MKL

Model	Values	ARE	SSE	HYBRID	EABS	MPSD	χ^2
Langmuir		27.34	0.06	1.63	0.77	33.94	0.19
q_{max} (mmol g^{-1})	0.711						
q_{max} (mg g^{-1})	290.0						
K_L (L mmol^{-1})	0.022						
R^2	0.9602						
Freundlich		21.92	0.05	0.92	0.64	27.22	0.27
K_F (mmol g^{-1} (L mmol^{-1})$^{1/n}$)	0.030						
n	1.847						
R^2	0.8679						
Temkin		33.29	0.06	1.92	0.75	44.44	0.26
K_T (L mmol^{-1})	0.689						
b_T (kJ mol^{-1})	24.024						
R^2	0.9338						
Redlich–Peterson		21.90	0.05	0.98	0.64	27.98	0.27
K_R (L g^{-1})	4.000						
β	0.460						
a_R (L mmol^{-1})	134.15						
R^2	0.8245						
Sips		18.56	0.02	0.64	0.41	28.57	0.15
q_{max} (mmol g^{-1})	0.960						
q_{max} (mg g^{-1})	391.7						
K_s (L mmol^{-1})	0.034						
$1/n$	0.674						
n	1.484						
R^2	0.9588						

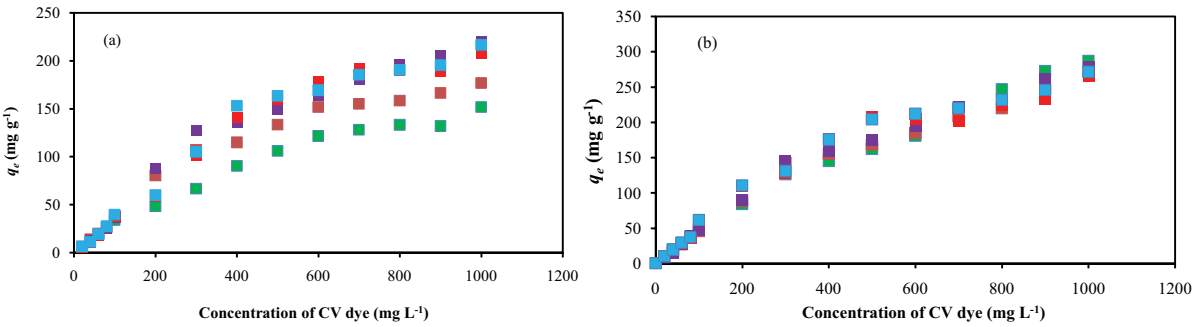

Fig. 12. Adsorption of CV on (a) MKL and (b) NaOH-MKL at 298 K (■), 313 K (■), 323 K (■), 333 K (■) and 343 K (■).

studies provide vital information in designing and planning of wastewater treatment plants because some plants are operated under warm temperature conditions. It is of importance to record that the amount of CV adsorbed on NaOH-MKL at temperatures above 298 K does not vary, a valuable condition to be considered for operation of effluent treatment plants (Table 6).

3.6. Regeneration and reusability of MKL and NaOH-MKL

In large scale wastewater treatment, it is imperative that the adsorbent chosen is reusable for the method to be cost-effective, thereby decreasing the demand for raw materials. Further, spent adsorbents if simply disposed without proper incineration not only contribute to landfill waste but could also be health hazards to human. Hence, one of the key factors in selecting a suitable adsorbent in wastewater treatment application is its potential to be regenerated and reused.

Herein, the spent adsorbents were tested with three solvents, that is, 0.1 M NaOH, 0.1 M HCl, and distilled water. A control experiment was also set up for each adsorbent using spent adsorbent without any prior treatment for comparison purpose. Fig. 13 shows that both MKL and

Table 5
Comparison of q_{max} of various adsorbents reported

Unmodified adsorbent	q_{max} (mg g^{-1})	Reference
MKL	208.1	This work
Lemongrass leaf	36.1	[49]
Artocarpus odoratissimus leaf	50.5	[50]
Calligonum comosum leaf	5.0	[51]
Spent tea leaf	114.9	[52]
Ananas comosus (pineapple) leaf	158.7	[53]
Calotropis procera leaf	4.1	[54]
Garcinia indica (Kokum) leaf	109.9	[55]
Quercus robur (Oak) leaf	41.2	[56]
Artocarpus heterophyllus (Jackfruit) leaf	43.4	[57]
Artocarpus odoratissimus (Tarap) core	217.0	[58]
Artocarpus altilis (Breadfruit) skin	145.8	[59]
Artocarpus odoratissimus leaf-based cellulose	239.0	[60]
Formosa papaya (*Carica papaya* L.) seed powder	86.0	[61]
Momordica charantia (bitter gourd) waste	244.8	[62]
Cucumis sativus peel	149.3	[63]
Parkia speciosa (Petai) pod	163.2	[64]
Sepia shells (cuttlefish bones)	218.7	[65]
Peat	108.0	[66]
Mycelial biomass of *Ceriporia lacerata*	239.3	[67]
Palm kernel fiber	95.4	[68]
Eichhornia crassipes (Water hyacinth)	322.6	[69]
Artocarpus camansi peel	275.0	[70]
Artocarpus odoratissimus (Tarap) skin	118.0	[71]
Modified or synthesized adsorbents		
NaOH modified MKL	391.7	This work
Yeast treated peat	18.0	[29]
Gum arabic-cl-poly(acrylamide) nanohydrogel	90.9	[72]
NaOH modified *Artocarpus odoratissimus* (Tarap) skin	195.0	[71]
Modified bentonites	74.1	[73]
TLAC/Chitosan composite	0.3	[74]
NaOH *Artocarpus camansi* peel	479.0	[70]
EDTA/graphene oxide functionalized corncob	203.9	[75]
Dendritic post-cross-linked resin	497.5	[76]
Oppositely twisted heat-treated halloysite	190.0	[77]
Silver nanoparticles immobilised on the activated carbon	87.2	[78]
ZSM-5 zeolite	141.8	[79]
Functionalized multi-walled carbon nanotubes	90.5	[80]
Chitosan aniline composite of peanut hull waste	100.6	[81]

its modified form were able to successfully adsorb CV dye even after five consecutive cycles. High adsorption efficiency was noted when the spent adsorbents were washed with base, maintaining >96% at the fifth cycle, clearly indicating the reusability of the spent adsorbents.

4. Conclusion

The performance of MKL and its modified form (NaOH-MKL), prepared by treatment with aqueous NaOH solution, toward CV dye adsorption indicates strong affinity of both adsorbents. More importantly, the modified form, NaOH-MKL, is found to be superior to MKL demonstrating improvement of both equilibrium and kinetics aspects of the transfer of CV dye to the adsorbent phase; 88% increase in adsorption capacity and 72% in the rate of mass transfer. Further, transfer of CV dye molecules from the solution phase to the adsorbent phase occurs favorably through a boundary layer according to the findings of the Webber–Morris intraparticle diffusion model.

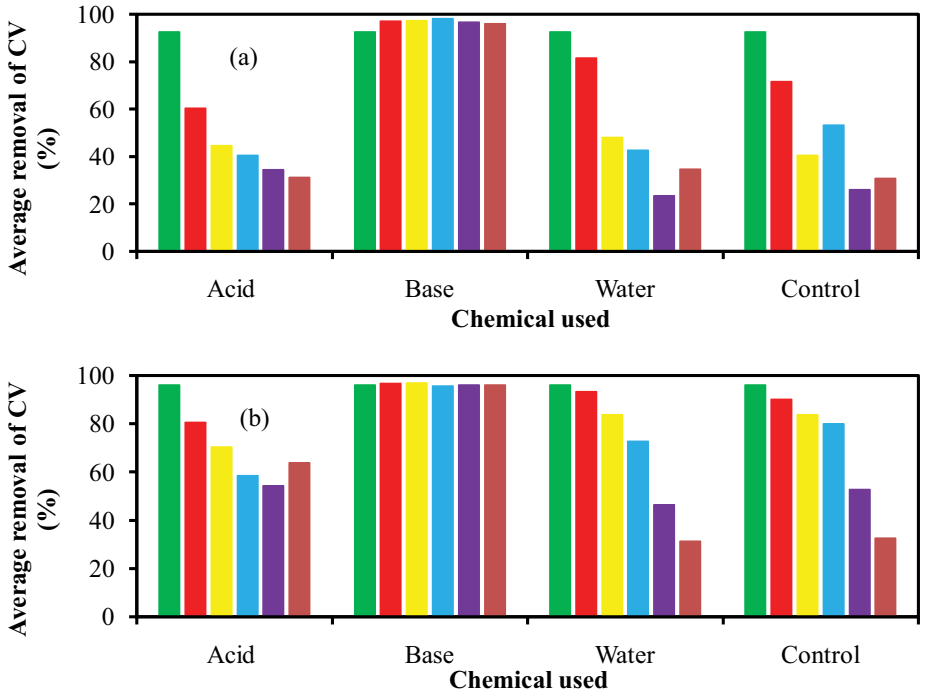

Fig. 13. Regeneration of (a) spent MKL and (b) spent NaOH-MKL for the adsorption of CV in five consecutive cycles [Cycles 0 (■), 1 (■), 2 (■), 3 (■), 4 (■), and 5 (■)].

Table 6
Extent of adsorption of CV dye on MKL and NaOH-MKL at different solution temperatures

	MKL	NaOH-MKL
Temperature (K)	q_{max} (mg g^{-1})	q_{max} (mg g^{-1})
298	208.08	391.70
313	191.76	367.19
323	244.79	367.19
333	244.79	367.19
343	244.79	367.19

Among the five isotherm models investigated, namely, Langmuir, Freundlich, Temkin, Redlich–Peterson, and Sips, the Sips isotherm is found to be the most suitable based on regression coefficient of non-linear curve fitting and error analyses of many standard types of error functions. Having the Sips adsorption isotherm satisfied is indicative of a combination of both the Langmuir and Freundlich characteristics. Another attractive feature is that MKL was found to be stable, maintaining its adsorption toward CV dye throughout pH 2–12 and exhibiting >90% adsorption of CV dye at 1.0 M NaCl. Except at pH 2, NaOH-MKL also showed that it is resilient to changes in pH with >90% dye removal from pH 4 to 12. Both spent adsorbents can be regenerated with aqueous 0.1 M NaOH solution, maintaining close to 100% adsorption of CV dye even at the fifth consecutive cycle, thus promoting their reuse and indicating the potential for practical applications with large volumes of CV dye solutions. Owing to favorable equilibrium and kinetics aspects of adsorption of CV on NaOH-MKL, the next logical step of this research would be to extend toward dynamic conditions and proto-type systems through optimization of relevant experimental conditions, with the goal of extending toward real situation for effective removal of CV dye from industrial effluents.

Acknowledgments

The authors acknowledge the continuous support of the Government of Negara Brunei Darussalam and the Universiti Brunei Darussalam (UBD), and thank the Geosciences Programme at UBD for helping with the SEM analyses.

References

[1] Y. Zhou, L. Zhang, Z. Cheng, Removal of organic pollutants from aqueous solution using agricultural wastes: a review, J. Mol. Liq., 212 (2015) 739–762.
[2] Z. Shamsollahi, A. Partovinia, Recent advances on pollutants removal by rice husk as a bio-based adsorbent: a critical review, J. Environ. Manage., 246 (2019) 314–323.
[3] S. Rangabhashiyam, S. Lata, P. Balasubramanian, Biosorption characteristics of methylene blue and malachite green from simulated wastewater onto *Carica papaya* wood biosorbent, Surf. Interfaces, 10 (2018) 197–215.
[4] A.A. Adeyemo, I.O. Adeoye, O.S. Bello, Adsorption of dyes using different types of clay: a review, Appl. Water Sci., 7 (2017) 543–568.
[5] J. Mo, Q. Yang, N. Zhang, W. Zhang, Y. Zheng, Z. Zhang, A review on agro-industrial waste (AIW) derived adsorbents for water and wastewater treatment, J. Environ. Manage., 227 (2018) 395–405.
[6] B. Cojocariu, A.M. Mocanu, G. Nacu, L. Bulgariu, Possible utilization of PET waste as adsorbent for orange g dye removal from aqueous media, Desal. Water Treat., 104 (2018) 338–345.

[7] Y.C. Lu, N. Priyantha, L.B.L. Lim, M. Suklueng, Toxic yellow cow dung powder (Auramine O dye) removal via *Ipomoea aquatica* waste, Desal. Water Treat., 181 (2020) 422–435.
[8] N.B. Singh, G. Nagpal, S. Agrawal, Rachna, Water purification by using adsorbents: a review, Environ. Technol. Innovation, 11 (2018) 187–240.
[9] G. Ravindiran, G.P. Ganapathy, J. Josephraj, A. Alagumalai, A critical insight into biomass derived biosorbent for bioremediation of dyes, ChemistrySelect, 4 (2019) 9762–9775.
[10] Z.N. Garba, I. Lawan, W. Zhou, M. Zhang, L. Wang, Z. Yuan, Microcrystalline cellulose (MCC) based materials as emerging adsorbents for the removal of dyes and heavy metals – a review, Sci. Total Environ., 717 (2019), doi: 10.1016/j.scitotenv.2019.135070.
[11] H.N. Tran, H.C. Nguyen, S.H. Woo, T.V. Nguyen, S. Vigneswaran, A. Hosseini-Bandegharaei, J. Rinklebe, A. Kumar Sarmah, A. Ivanets, G.L. Dotto, T.T. Bui, R.S. Juang, H.P. Chao, Removal of various contaminants from water by renewable lignocellulose-derived biosorbents: a comprehensive and critical review, Crit. Rev. Environ. Sci. Technol., 49 (2019) 2155–2219.
[12] L.B.L. Lim, N. Priyantha, X. Han, N. Afiqah, H. Mohamad, Enhancement of adsorption characteristics of Methyl violet 2B dye through NaOH treatment of *Cucumis melo* var. cantalupensis (rock melon) skin, Desal. Water Treat., 180 (2020) 336–348.
[13] H. Shayesteh, A. Rahbar-Kelishami, R. Norouzbeigi, Evaluation of natural and cationic surfactant modified pumice for congo red removal in batch mode: kinetic, equilibrium, and thermodynamic studies, J. Mol. Liq., 221 (2016) 1–11.
[14] M. Choudhary, R. Kumar, S. Neogi, Activated biochar derived from *Opuntia ficus*-indica for the efficient adsorption of malachite green dye, Cu^{+2} and Ni^{+2} from water, J. Hazard. Mater., 392 (2020), doi: 10.1016/j.jhazmat.2020.122441.
[15] Q.U. Ain, H. Zhang, M. Yaseen, U. Rasheed, K. Liu, S. Subhan, Z. Tong, Facile fabrication of hydroxyapatite-magnetite-bentonite composite for efficient adsorption of Pb(II), Cd(II), and crystal violet from aqueous solution, J. Cleaner Prod., 247 (2020), doi: 10.1016/j.jclepro.2019.119088.
[16] S.E. Karekar, K.A. Gondhalekar, D.K. Chandre, S.H. Sonawane, D. V. Pinjari, Acoustic cavitation assisted preparation of poly(acrylic acid)-halloysite nanoclay hydrogel for removal of Auramine O dye from effluent, Curr. Environ. Eng., 5 (2018) 47–57.
[17] Y. Lu, N. Priyantha, L.B.L. Lim, *Ipomoea aquatica* roots as environmentally friendly and green adsorbent for efficient removal of Auramine O dye, Surf. Interfaces, 20 (2020), doi: 10.1016/j.surfin.2020.100543.
[18] L.B.L. Lim, N. Priyantha, Y. Lu, N.A.H. Mohamad Zaidi, Adsorption of heavy metal lead using *Citrus grandis* (Pomelo) leaves as low-cost adsorbent, Desal. Water Treat., 166 (2019) 44–52.
[19] S. Hussain, K.P. Anjali, S.T. Hassan, P.B. Dwivedi, Waste tea as a novel adsorbent: a review, Appl. Water Sci., 8 (2018), doi: 10.1007/s13201-018-0824-5.
[20] Y. Tang, Y. Li, Y. Zhao, Q. Zhou, Y. Peng, Enhanced removal of methyl violet using NaOH-modified *C. camphora* leaves powder and its renewable adsorption, Desal. Water Treat., 98 (2017) 306–314.
[21] M.R.R. Kooh, M.K. Dahri, L.B.L. Lim, Removal of methyl violet 2B dye from aqueous solution using *Nepenthes rafflesiana* pitcher and leaves, Appl. Water Sci., 7 (2017) 3859–3868.
[22] N.A.H.M. Zaidi, L.B.L. Lim, A. Usman, M.R.R. Kooh, Efficient adsorption of malachite green dye using *Artocarpus odoratissimus* leaves with artificial neural network modelling, Desal. Water Treat., 101 (2018) 313–324.
[23] A.G. Adeniyi, J.O. Ighalo, Biosorption of pollutants by plant leaves: an empirical review, J. Environ. Chem. Eng., 7 (2019), doi: 10.1016/J.JECE.2019.103100.
[24] L. Bulgariu, L.B. Escudero, O.S. Bello, M. Iqbal, J. Nisar, K.A. Adegoke, F. Alakhras, M. Kornaros, I. Anastopoulos, The utilization of leaf-based adsorbents for dyes removal: a review, J. Mol. Liq., 276 (2019) 728–747.
[25] A. Asheeba, L.B.L. Lim, C. Mei, N. Priyantha, Application of *Dimocarpus longan* ssp. malesianus leaves in the sequestration of toxic brilliant green dye, Desal. Water Treat., 189 (2020) 428–439.
[26] M. Balabanova, L. Popova, R. Tchipeva, Dyes in dermatology, Disease-a-Month, 50 (2004) 270–279.
[27] R. Docampo, S.N.J. Moreno, The metabolism and mode of action of gentian violet, Drug Metab. Rev., 22 (1990) 161–166.
[28] N.A. Littlefield, B.N. Blackwell, C.C. Hewitt, D.W. Gaylor, Chronic toxicity and carcinogenicity studies of gentian violet in mice, Toxicol. Sci., 5 (1985) 902–912.
[29] T. Zehra, N. Priyantha, L.B.L. Lim, Removal of crystal violet dye from aqueous solution using yeast-treated peat as adsorbent: thermodynamics, kinetics, and equilibrium studies, Environ. Earth Sci., 75 (2016), doi: 10.1007/s12665-016-5255-8.
[30] Y. Lu, L.B.L. Lim, N. Priyantha, Chemical modification of pomelo leaves as a simple and effective way to enhance adsorption toward methyl violet dye, Desal. Water Treat., 197 (2020) 379–391.
[31] D. Trache, M.H. Hussin, C.T. Hui Chuin, S. Sabar, M.R.N. Fazita, O.F.A. Taiwo, T.M. Hassan, M.K.M. Haafiz, Microcrystalline cellulose: isolation, characterization and bio-composites application—a review, Int. J. Biol. Macromol., 93 (2016) 789–804.
[32] D. Schwantes, A.C. Gonçalves, G.F. Coelho, M.A. Campagnolo, D.C. Dragunski, C.R.T. Tarley, A.J. Miola, E.A.V. Leismann, Chemical modifications of cassava peel as adsorbent material for metals ions from wastewater, J. Chem., 2016 (2016), doi:10.1155/2016/3694174.
[33] M.R.R. Kooh, L.B.L. Lim, L.H. Lim, J.M.R.S. Bandara, Batch adsorption studies on the removal of malachite green from water by chemically modified *Azolla pinnata*, Desal. Water Treat., 57 (2016) 14632–14646.
[34] M.K. Dahri, M. Kooh, L. Lim, *Casuarina equisetifolia* cone as sustainable adsorbent for removal of Malachite green dye from aqueous solution using batch experiment method, Moroccan J. Chem., 6 (2018) 480–491.
[35] A. Aichour, H. Zaghouane-Boudiaf, Highly brilliant green removal from wastewater by mesoporous adsorbents: kinetics, thermodynamics and equilibrium isotherm studies, Microchem. J., 146 (2019) 1255–1262.
[36] S.K. Brar, N. Wangoo, R.K. Sharma, Enhanced and selective adsorption of cationic dyes using novel biocompatible self-assembled peptide fibrils, J. Environ. Manage., 255 (2020), doi: 10.1016/j.jenvman.2019.109804.
[37] L.B.L. Lim, N. Priyantha, S. Amanina, A. Latip, Y. Chen, A. Hanif, Converting *Hylocereus undatus* (white dragon fruit) peel waste into a useful potential adsorbent for the removal of toxic Congo red dye, Desal. Water Treat., 185 (2020) 307–317.
[38] S. Lagergren, About the theory of so-called adsorption of soluble substances, K. Sven. Vetenskapsakad. Handl., 24 (1898) 1–39.
[39] G. McKay, Y.S. Ho, Pseudo-second order model for sorption processes, Process Biochem., 34 (1999) 451–465.
[40] P. Anurudda, N. Priyantha, L.B.L. Lim, Biosorption of heavy metal ions on peel of *Artocarpus nobilis* fruit: 2. Improvement of biosorption capacities of Ni(II) through different modifications, Desal. Water Treat., 185 (2020) 226–236.
[41] R. Saadi, Z. Saadi, R. Fazaeli, N.E. Fard, Monolayer and multilayer adsorption isotherm models for sorption from aqueous media, Korean J. Chem. Eng., 32 (2015) 787–799.
[42] E.I. Unuabonah, M.O. Omorogie, N.A. Oladoja, 5 - Modeling in Adsorption: Fundamentals and Applications, Composite Nanoadsorbents - Micro Nano Technol., (2019) 85–118. doi:10.1016/b978-0-12-814132-8.00005-8.
[43] I. Langmuir, The adsorption of gases on plane surfaces of glass, mica and platinum, J. Am. Chem. Soc., 40 (1918) 1361–1403.
[44] H. Freundlich, Over the adsorption in the solution, J. Phys. Chem., 57 (1906) 385–470.
[45] M.J. Temkin, V. Pyzhev, Kinetics of ammonia synthesis on promoted iron catalysts, Acta Physiochim., 12 (1940).
[46] O. Redlich, D.L. Peterson, A useful adsorption isotherm, J. Phys. Chem., 63 (1959), doi: 0.1021/j150576a611.
[47] R. Sips, Combined form of Langmuir and Freundlich equations, J. Phys. Chem., 16 (1948) 490–495.

[48] N. Tzabar, H.J.M. ter Brake, Adsorption isotherms and Sips models of nitrogen, methane, ethane, and propane on commercial activated carbons and polyvinylidene chloride, Adsorption, 22 (2016) 901–914.
[49] K.N.A. Putri, A. Keereerak, W. Chinpa, Novel cellulose-based biosorbent from lemongrass leaf combined with cellulose acetate for adsorption of crystal violet, Int. J. Biol. Macromol., 156 (2020) 762–772.
[50] L.B.L. Lim, N. Priyantha, H.H. Cheng, N.A.H. Mohamad Zaidi, Adsorption characteristics of *Artocarpus odoratissimus* leaf toward removal of toxic Crystal violet dye: isotherm, thermodynamics and regeneration studies, J. Environ. Biotechnol., 4 (2016) 32–40.
[51] G. Alsenani, Studies on adsorption of crystal violet dye from aqueous solution onto calligonum comosum leaf powder (CCLP), J. Am. Sci., 9 (2013) 30–35.
[52] A. Bajpai, A. Jain, Equilibrium and thermodynamic studies for adsorption of crystal violet onto spent tea leaves (STL), Water J., 4 (2012) 52–71.
[53] S. Neupane, S.T. Ramesh, R. Gandhimathi, P. V. Nidheesh, Pineapple leaf (*Ananas comosus*) powder as a biosorbent for the removal of crystal violet from aqueous solution, Desal. Water Treat., 54 (2015) 2041–2054.
[54] H. Ali, S.K. Muhammad, Biosorption of crystal violet from water on leaf biomass of *Calotropis procera*, J. Environ. Sci. Technol., 1 (2008) 143–150.
[55] P. Jamdade, S. Ubale, Adsorptive removal of Crystal Violet from aqueous solution by Kokum (*Garcinia indica*) leaf powder: equilibrium and thermodynamic studies, J. Emerg. Technol. Innovation Res., 6 (2019) 1436–1439.
[56] M. Sulyman, J. Namiesnik, A. Gierak, Utilization of new activated carbon derived from Oak leaves for removal of crystal violet from aqueous solution, Pol. J. Environ. Stud., 23 (2014) 2223–2232.
[57] P. Das Saha, S. Chakraborty, S. Chowdhury, Batch and continuous (fixed-bed column) biosorption of crystal violet by *Artocarpus heterophyllus* (jackfruit) leaf powder, Colloids Surf., B, 92 (2012) 262–270.
[58] M.K. Dahri, M.R.R. Kooh, L.B.L. Lim, *Artocarpus odoratissimus* (Tarap) core as an adsorbent for the removal of crystal violet dye from aqueous solution, J. Mater. Environ. Sci., 8 (2017) 3706–3717.
[59] L.B.L. Lim, N. Priyantha, N.H.M. Mansor, *Artocarpus altilis* (breadfruit) skin as a potential low-cost biosorbent for the removal of crystal violet dye: equilibrium, thermodynamics and kinetics studies, Environ. Earth Sci., 73 (2015) 3239–3247.
[60] N.A.H.M. Zaidi, L.B.L. Lim, A. Usman, *Artocarpus odoratissimus* leaf-based cellulose as adsorbent for removal of methyl violet and crystal violet dyes from aqueous solution, Cellulose, 25 (2018) 3037–3049.
[61] F.A. Pavan, E.S. Camacho, E.C. Lima, G.L. Dotto, V.T.A. Branco, S.L.P. Dias, Formosa papaya seed powder (FPSP): preparation, characterization and application as an alternative adsorbent for the removal of crystal violet from aqueous phase, J. Environ. Chem. Eng., 2 (2014) 230–238.
[62] L.B.L. Lim, N. Priyantha, J. Mek, A. Hazirah, M. Zaidi, N.A.H.M. Zaidi, Potential use of *Momordica charantia* (bitter gourd) waste as a low-cost adsorbent to remove toxic crystal violet dye, Desal. Water Treat., 82 (2017) 121–130.
[63] S. Shakoor, A. Nasar, Utilization of *Cucumis sativus* peel as an eco-friendly biosorbent for the confiscation of crystal violet dye from artificially contaminated wastewater, Anal. Chem. Lett., 9 (2019) 1–19.
[64] L.B.L. Lim, N. Priyantha, H.H. Cheng, N. Afiqah, H. Mohamad, *Parkia speciosa* (Petai) pod as a potential low-cost adsorbent for the removal of toxic crystal violet dye, Sci. Bruneiana, 15 (2016) 99–106.
[65] K.Z. Elwakeel, A.M. Elgarahy, G.A. Elshoubaky, S.H. Mohammad, Microwave assist sorption of crystal violet and Congo red dyes onto amphoteric sorbent based on upcycled Sepia shells, J. Environ. Health Sci. Eng., 18 (2020) 35–50.
[66] H.I. Chieng, L.B.L. Lim, N. Priyantha, D.T.B. Tennakoon, Sorption characteristics of peat of Brunei Darussalam III: equilibrium and kinetics studies on adsorption of crystal violet (CV), Int. J. Earth Sci. Eng., 6 (2013) 791–801.
[67] Y. Lin, X. He, G. Han, Q. Tian, W. Hu, Removal of Crystal Violet from aqueous solution using powdered mycelial biomass of *Ceriporia lacerata* P2, J. Environ. Sci., 23 (2011) 2055–2062.
[68] G.O. El-Sayed, Removal of methylene blue and crystal violet from aqueous solutions by palm kernel fiber, Desalination, 272 (2011) 225–232.
[69] M.R. Kulkarni, T. Revanth, A. Acharya, P. Bhat, Removal of Crystal Violet dye from aqueous solution using water hyacinth: equilibrium, kinetics and thermodynamics study, Resour. Technol., 3 (2017) 71–77.
[70] H.I. Chieng, L.B.L. Lim, N. Priyantha, Enhancement of crystal violet dye adsorption on *Artocarpus camansi* peel through sodium hydroxide treatment, Desal. Water Treat., 58 (2017) 320–331.
[71] L.B.L. Lim, N. Priyantha, T. Zehra, C.W. Then, C.M. Chan, Adsorption of crystal violet dye from aqueous solution onto chemically treated *Artocarpus odoratissimus* skin: equilibrium, thermodynamics, and kinetics studies, Desal. Water Treat., 57 (2016) 10246–10260.
[72] G. Sharma, A. Kumar, M. Naushad, A. García-Peñas, A.H. Al-Muhtaseb, A.A. Ghfar, V. Sharma, T. Ahamad, F.J. Stadler, Fabrication and characterization of Gum arabic-cl-poly(acrylamide) nanohydrogel for effective adsorption of crystal violet dye, Carbohydr. Polym., 202 (2018) 444–453.
[73] N.R.E. Radwan, M. Hagar, K. Chaieb, Adsorption of crystal violet dye on modified bentonites, Asian J. Chem., 28 (2016) 1643–1647.
[74] H. Jayasantha Kumari, P. Krishnamoorthy, T.K. Arumugam, S. Radhakrishnan, D. Vasudevan, An efficient removal of crystal violet dye from waste water by adsorption onto TLAC/Chitosan composite: a novel low cost adsorbent, Int. J. Biol. Macromol., 96 (2017) 324–333.
[75] H. Wang, X. Lai, W. Zhao, Y. Chen, X. Yang, X. Meng, Y. Li, Efficient removal of crystal violet dye using EDTA/graphene oxide functionalized corncob: a novel low cost adsorbent, RSC Adv., 9 (2019) 21996–22003.
[76] X. Yuan, F. Zhou, R. Man, J. Huang, Dendritic post-cross-linked resin for the adsorption of crystal violet from aqueous solution, J. Chem. Thermodyn., 130 (2019) 235–242.
[77] A.A. Krasilin, D.P. Danilovich, E.B. Yudina, S. Bruyere, J. Ghanbaja, V.K. Ivanov, Crystal violet adsorption by oppositely twisted heat-treated halloysite and pecoraite nanoscrolls, Appl. Clay Sci., 173 (2019) 1–11.
[78] A.H. AbdEl-Salam, H.A. Ewais, A.S. Basaleh, Silver nanoparticles immobilised on the activated carbon as efficient adsorbent for removal of crystal violet dye from aqueous solutions. A kinetic study, J. Mol. Liq., 248 (2017) 833–841.
[79] G.V. Brião, S.L. Jahn, E.L. Foletto, G.L. Dotto, Adsorption of crystal violet dye onto a mesoporous ZSM-5 zeolite synthetized using chitin as template, J. Colloid Interface Sci., 508 (2017) 313–322.
[80] V. Sabna, S.G. Thampi, S. Chandrakaran, Adsorption of crystal violet onto functionalised multi-walled carbon nanotubes: equilibrium and kinetic studies, Ecotoxicol. Environ. Saf., 134 (2016) 390–397.
[81] N. Tahir, H.N. Bhatti, M. Iqbal, S. Noreen, Biopolymers composites with peanut hull waste biomass and application for Crystal Violet adsorption, Int. J. Biol. Macromol., 94 (2017) 210–220.

Supplementary information

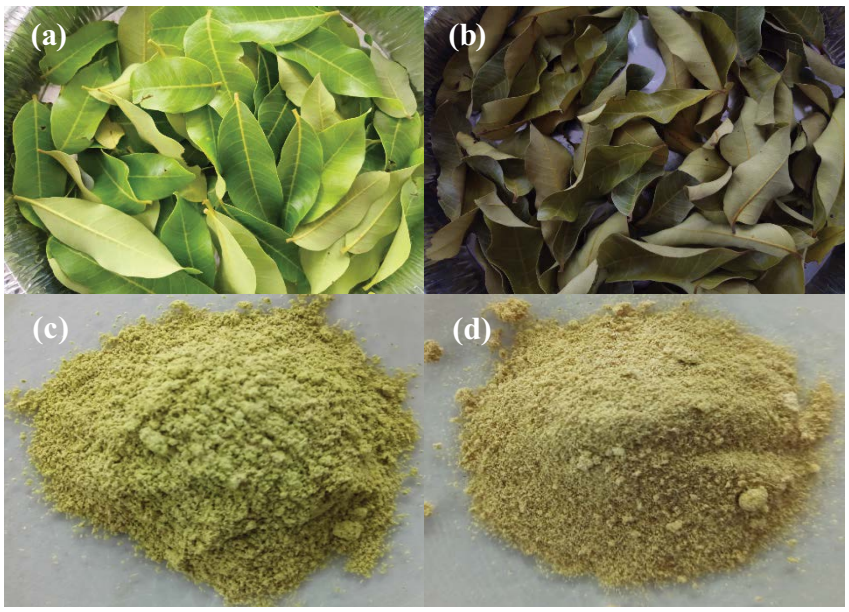

Fig. S1. (a) Freshly collected MKL, (b) oven dried MKL, (C) powdered MKL, and (d) NaOH-modified MKL.

Error functions:

$$\text{EABS: } \sum_{i=1}^{p}\left|q_{e,\text{meas}}-q_{e,\text{calc}}\right| \quad (1)$$

$$\text{ARE: } \frac{100}{p}\sum_{i=1}^{p}\left|\frac{q_{e,\text{meas}}-q_{e,\text{calc}}}{q_{e,\text{calc}}}\right|_i \quad (2)$$

$$\text{MPSD: } \sqrt[100]{\frac{1}{p-n}\sum_{i=1}^{p}\left(q_{e,\text{meas}}-q_{e,\text{calc}}\right)^2} \quad (3)$$

$$\text{SSE: } \sum_{i=1}^{n}\left(q_{e,\text{calc}}-q_{e,\text{meas}}\right)_i^2 \quad (4)$$

$$\text{HYBRID: } \frac{100}{n-p}\sum_{i=1}^{n}\left[\frac{\left(q_{e,\text{meas}}-q_{e,\text{calc}}\right)^2}{q_{e,\text{meas}}}\right]_i \quad (5)$$

$$\chi^2\text{: } \sum_{i=1}^{p}\frac{\left(q_{e,\text{meas}}-q_{e,\text{calc}}\right)^2}{q_{e,\text{meas}}} \quad (6)$$

Here $q_{e,\text{meas}}$ is the experimental value, while $q_{e,\text{calc}}$ is the value calculated from the isotherm models and p is the number of observations in the experiment.